Optical emission spectroscopic studies on laser ablated zinc oxide plasma

K. J. Saji, N. V. Joshy, and M. K. Jayaraj[a)]
Optoelectronic Devices Laboratory, Department of Physics, Cochin University of Science and Technology, Kochi-682 022, India

(Received 17 December 2005; accepted 1 June 2006; published online 23 August 2006)

Optical emission spectroscopic studies were carried out on the plasma produced by ablation of zinc oxide target using the third harmonic (355 nm) of *Q*-switched Nd:YAG laser, in vacuum and at three different ambient gas (oxygen) pressures. The spatial variations of electron density (N_e) and electron temperature (T_e) were studied up to a distance of 20 mm from the target surface. The kinematics of the emitted particles and the expansion of the plume edge are discussed. The optimum conditions favorable for the formation of high quality zinc oxide thin films are thereby suggested. © *2006 American Institute of Physics*. [DOI: 10.1063/1.2266260]

I. INTRODUCTION

Wide-band-gap semiconductors have attracted a great deal of attention because of the immense commercial interest in developing practical short-wavelength semiconductor diode lasers (SDLs) for the huge market needs. Zinc oxide (ZnO) being a wide-band-gap (3.37 eV), nontoxic, and abundant semiconductor has numerous applications in diverse areas such as facial powders, piezoelectric transducers, varistors, phosphors, surface acoustic wave (SAW) devices,[1] waveguides, and transparent conducting films. Recently there has been much interest in the growth and optical characteristics of ZnO films for ultraviolet (UV) and blue light emitting device applications. ZnO films generally exhibit *n*-type conductivity which can further be improved and stabilized by doping with Al or Ga.[2–4] The high conductivity, together with broad optical transparency, has prompted extensive investigations of ZnO films as transparent electrodes for flat-panel displays,[5] thin film transistors,[6] and solar cells.[7]

ZnO films have been grown by a variety of methods, such as radio-frequency (rf) and direct-current (dc) sputtering,[3,8,9] chemical vapor deposition,[10] spray pyrolysis,[11] electron-cyclotron-resonance-assisted molecular beam epitaxy,[12] and pulsed laser deposition (PLD).[2,13,14]

In contrast to the extensive literature relating to ZnO films produced by PLD and their properties, there appears to have relatively little effort directed towards characterization of the ablation plume from which such films are produced.[15,16] Different mechanisms involved during a laser ablation process are rather complex and the expansion dynamics of the plasma plume, in vacuum or in a background gas, are still not fully understood. In this article we report results of optical emission spectroscopic studies of ZnO plasma plume accompanying pulsed laser ablation. Analysis of these data provides information on the nature of the ejected particles, their density, and temperature in the vicinity of the target surface.

[a)]Author to whom correspondence should be addressed; FAX: +91 484 2577595; electronic mail: mkj@cusat.ac.in

II. EXPERIMENTAL SETUP

A Nd:YAG (yttrium aluminum garnet) laser (Quanta Ray, Spectra Physics) operating at 355 nm, 10 Hz repetition rate, was used for the ablation of ZnO (99.95% pure, sintered at 900 °C for 12 h). The target was mounted inside a stainless steel vacuum chamber and rotated at a constant rate. The laser beam was focused onto the target using a quartz lens ($f=30$ cm) at an angle of 45° with respect to the target normal. The spot size of the laser was adjusted to be of 2 mm diameter. The target and chamber were kept at ground potential. The plume emanating from the target surface was focused using a spherical lens ($f=50$ mm) onto an optic fiber bundle, the other end of which coupled optically to the entrance slit of a monochromator (Triax 320, Jobin Yvon, 1200 grooves/mm grating). The wavelength dispersed spectrum of the plume was imaged using a charge coupled device (CCD) (Spectrum One 2000, 1024×256 pixels). The spectra were taken along the propagation direction of the plume up to 20 mm distance from the target surface both in vacuum ($\sim10^{-6}$ mbar) and at three different ambient gas (oxygen) pressures. The laser energy was fixed at 10 mJ throughout this investigation. The CCD was triggered externally using a voltage pulse from the laser controller and interfaced with a personal computer (PC) using general purpose interface bus (GPIB) cable for storage of data and subsequent processing.

III. RESULTS AND DISCUSSION

A. Electron density and temperature

The two mercury emission lines at 578.88 and 576.75 nm (Fig. 1) were used for the determination of resolution ($\Delta\lambda$) of the spectrometer,[17]

$$\Delta\lambda = \frac{(\mathrm{FWHM})}{a}\times\Delta A, \tag{1}$$

where full width at half maximum (FWHM) of 576.75 nm line of mercury is about 0.065 nm, a is the measured wavelength separation between the two peaks (2.13 nm), and ΔA is the standard wavelength difference of mercury lines (579.06−576.96=2.1 nm). Our spectrometer resolution obtained from the above equation is 0.064 nm.

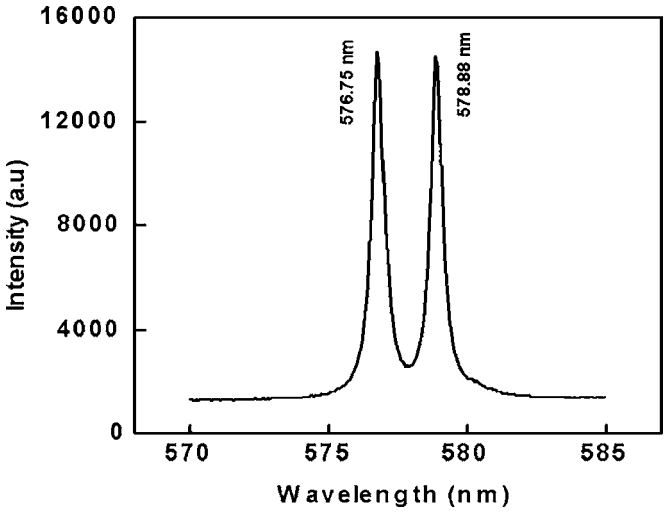

FIG. 1. Emission spectra of Hg.

The spectra arising from different atomic and ionic species in the plume during the ablation were recorded in the wavelength range of 350–850 nm. Strong emission lines of neutral zinc (Zn I), singly ionized zinc (Zn II), and neutral oxygen (O I) were obtained. Figure 2 shows the wavelength dispersed emission spectrum of the plume accompanying the ablation of the ZnO target in vacuum at laser pulse energy of 10 mJ and recorded at a distance of 6 mm from the target surface.

One of the most powerful spectroscopic techniques to determine the electron density is by measuring Stark broadened line profiles of isolated atoms or singly charged ions. For nonhydrogenic ions, Stark broadening is predominantly by electron impact. Since the perturbation caused by the ions is negligible compared to that due to electrons, the FWHM of the Stark broadened lines $\Delta\lambda_{1/2}$ is related to electron density by the expression[18]

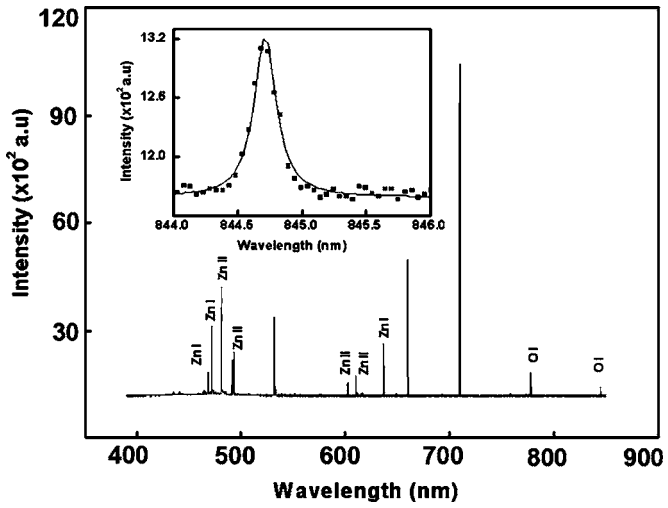

FIG. 2. Emission spectra of the ZnO plasma plume produced by 10 mJ, 355 nm laser pulse under vacuum. Emission data collected at distance 6 mm from the target. Inset shows a typical Stark broadened profile of 844.41 nm O I line and the Lorentzian fit.

$$\Delta\lambda_{1/2} = 2W\left(\frac{N_e}{10^{16}}\right)A^0, \tag{2}$$

where N_e is the electron density in cm^{-3}, and W is the electron impact parameter which is independent of electron density but at the same time a slowly varying functions of electron temperature. The Stark broadened emission line profile is generally Lorentzian and the spectral lines obtained in the present study (inset Fig. 2) fit well with the typical Lorentzian profile.

The approximate electron temperature was calculated by the method of Boltzmann plot[19] and was employed for the evaluation of electron impact parameter W. Since the value of W is not very much affected by the variations in T_e, it is presumed that the electron density N_e calculated by this method gives fairly good result. The 844.67 nm emission line of O I was used for electron density calculations.

For accurate evaluation of T_e, the ratio of line intensities from successive ionization stages of the same element is preferred over Boltzmann plot method. In local thermodynamic equilibrium, the ratio of line intensities from successive ionization stages of the same element is given by[18]

$$\frac{I'}{I} = \left(\frac{f'g'\lambda^3}{fg\lambda'^3}\right)(4\pi^{3/2}a_0{}^3N_e)\left(\frac{kT_e}{E_H}\right)^{3/2} \times\exp\left(-\frac{E'+E_\infty-E-\Delta E_\infty}{kT_e}\right), \tag{3}$$

where the primed symbols represent the lines of the atom with higher ionization stage, f is the oscillator strength, g is the statistical weight, a_0 is the Bohr radius, E_H is the ionization energy of the hydrogen atom, E the excitation energy, and ΔE_∞ is the correction to the ionization energy E_∞ of the lower ionization stage due to plasma interactions. The correction factor in the ionization energy is given by

$$\Delta E_\infty = 3z\frac{e^2}{4\pi\varepsilon_0}\left(\frac{4\pi N_e}{3}\right)^{1/3}, \tag{4}$$

where $z=2$ for the lower ionization stage.

For temperature calculations the line intensities corresponding to emission lines of 480.94 and 491.16 nm, respectively, of Zn I and Zn II have been used. The optical data required for the above calculations were taken from Ref. 18 and NIST atomic spectra database.[20]

The line shape analysis of different species was performed at different distances from the target surface. The spatial variations of electron density and electron temperature give an insight into the basic ionization processes taking place during the pulsed laser ablation. The estimation of electron temperature and electron density of the plasma plume was carried out for distances up to 20 mm from the target surface in a time-integrated manner. The spatial dependence of electron temperature and electron density of the plume is given in Figs. 3 and 4. The temperature and density exhibited a decreasing behavior with distance. With increasing distance from the target surface, the electron temperature varied from 2.43 eV at 1 mm to 1.6 eV at 11 mm and there-

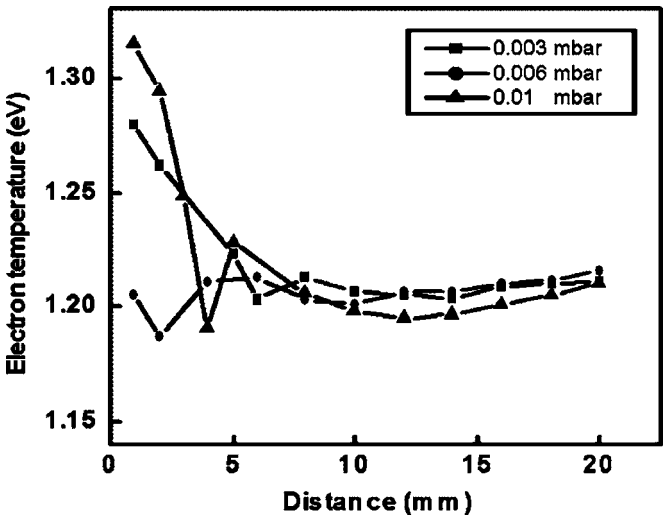

FIG. 3. Variation of electron temperature with distance from the target surface for different ambient gas pressures.

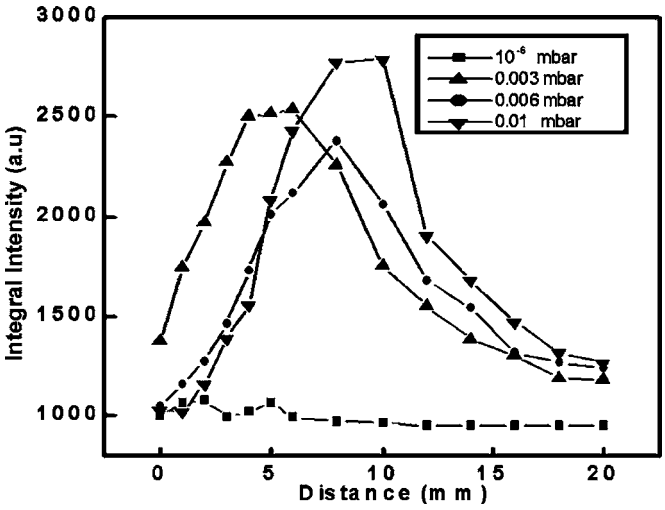

FIG. 5. Variation of integral intensity of 844.41 nm line of O I with distance from target surface. Integral intensity of O I without oxygen ambient gas is very small and almost insensitive of distance from the target.

after maintained steady behavior while electron density variation is about 1×10^{17} cm^{-3} over a distance of 20 mm from the target surface.

The electron temperature is found to decrease with increase in ambient gas pressure; however, the variation is small as expected. The increase in the ambient gas pressure will cause the collision of the ablated species with the oxygen atoms at the plume edge. This could cause a small reduction in plume expansion rate. As the plume starts expanding in an adiabatic manner from the target surface the decrease of N_e and T_e can be expected in the ablation of ZnO, quite like the case of exponential decrease reported in the ablation of pure metal targets.[21,22] The steady nature of T_e from about 10 mm distance indicates that the cooling due to adiabatic expansion is compensated by energy released during recombination of ions and electrons within the plume.

It is interesting to note that in the vicinity of 20 mm distance from the target surface there is a small tendency for T_e to increase. This could be due to the fact that at this distance, the adjoint mass of the ambient gas at the plume edge impedes the plume expansion, resulting in a large deviation from the free expansion when the mass of the gas surrounding the leading edge of the plume becomes comparable with the plume mass.[23] This impedance in the plume expansion could cause a redistribution of kinetic and thermal energies between the plume and ambient gas leading to a transfer of particle flux velocity into plume thermal energy, resulting in plume heating.[24]

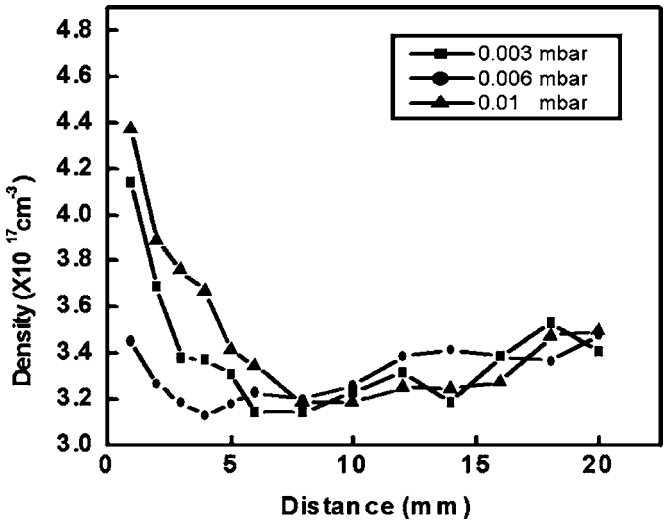

FIG. 4. Variation of electron density with distance from the target surface for different ambient gas pressures.

Figure 4 shows the variation of electron density with distance for three different ambient gas pressures. It exhibits rapidly decreasing behavior within short distances from the target surface and then remains more or less steady. Similar to the observation of T_e in the vicinity of 20 mm, N_e also shows a feeble upward trend. The dependence of N_e with background gas pressure is significant only in the regions closer to the target surface.

B. Intensity variation with pressure

The integrated emission intensity of O I line (844.41 nm) as a function of distance from the target surface is shown in the Fig. 5. The integrated yield has been obtained by integrating the whole area under the emission profile. This gives a measure of the amount of excited species within the plume, arriving at a given point.

The integral intensity of O I emission, generated during the ablation at various pressures of ambient gas, showed steady increase up to 10 mm distance from the target and then a monotonic decrease with further increase in distance. This is due to the increase in the excitation of oxygen atoms by the collision with the particles in the plume in the early stage of plume expansion. While in the later stage, the collision probability decreases due to the increase in the mean free path and hence the observed decrease in intensity. However, it should be noted that the increase in oxygen pressure increases the emission intensities. In the absence of ambient gas, oxygen line intensities were found to be very small and insensitive to distance variations. The integral intensities of

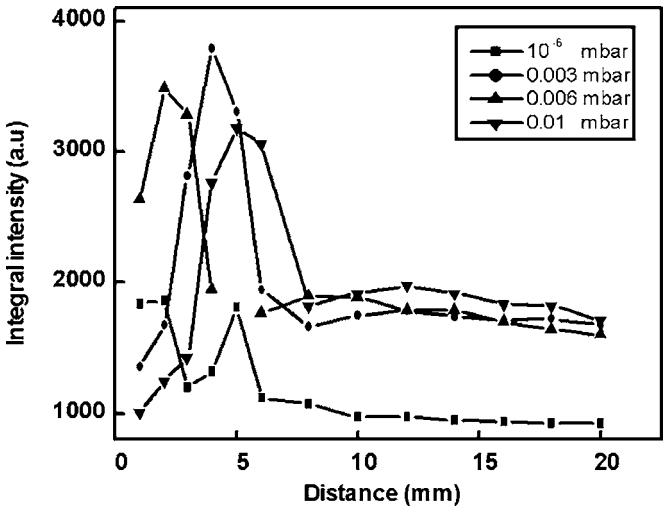

FIG. 6. Variation of integral intensity of 636.3 nm line of Zn I with distance from target surface. Increasing the ambient gas pressure increases the populations of excited Zn I.

the emission lines of both Zn I and Zn II (Figs. 6 and 7) exhibited a steady behavior from around 10 mm distances from the target surface.

The spatial variations of the integral intensity of the species in the plume (Figs. 5–7) show that density of zinc ions is manyfold large compared to oxygen and neutral zinc when ablated under high vacuum. Hence ZnO thin films with 1:1 stoichiometry cannot be expected under this condition, in agreement with the observations of Claeyssens *et al.*[25] Increase in oxygen pressure enhanced the emission line intensities of the neutral Zn and neutral oxygen while the emission line intensities of Zn ions decreased. This could be attributed to the fact that increase in pressure will decrease the mean free path of particles in the plume, thereby increasing the probability of collision of Zn ions with electrons in the plume. This will enhance the rate of electron-ion recombination, leading to the increase in the number of excited neutral zinc atoms.

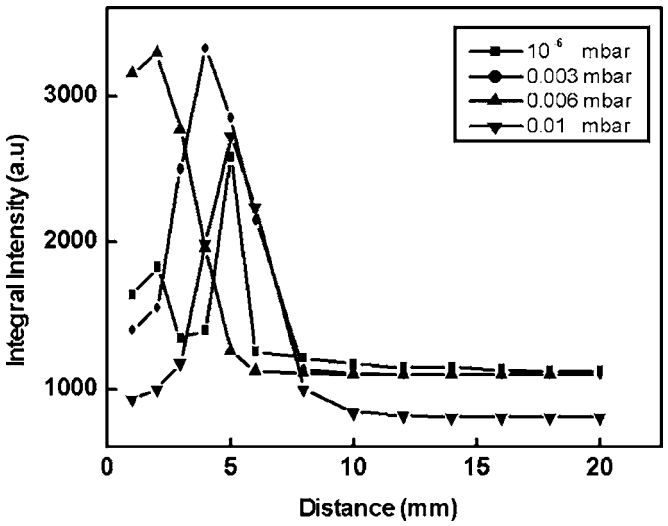

FIG. 7. Variation of integral intensity of 491.16 nm line of Zn II with distance from target surface. The increase in ambient gas pressure decreases the population of excited Zn II after 8 mm distance from the target.

The steady behavior of electron density, electron temperature and integral intensities of Zn and Zn ions, and high oxygen line intensities above 10 mm distance from the target surface suggest that high quality ZnO thin films can be expected when substrate is placed beyond this distance. However, the reports show that stoichiometric and crystalline films are formed at a few centimeters away from the target surface.[26] Even at relatively low laser intensities near the threshold for ablation, it has been observed that the ablated materials are significantly ionized,[27,28] and the ions in the plasma plume can have energies ranging up to several hundred eV.[29] So at small target to substrate separation there is the chance of sputtering from the substrate by these highly energetic particles and thereby affecting the qualities of the films deposited. Hence for proper nucleation and adherence and thereby for the formation of crystalline thin films, larger target to substrate distance and heating of substrate are suggested.

IV. CONCLUSION

The electron temperature and electron density in ZnO plasma show similar spatial behavior. Both decrease with distance from the target surface and become more or less steady from 10 mm distance from the target with electron temperature being at 1.2 eV and electron density at 3.2×10^{17} cm^{-3}. A small but significant rise in both N_e and T_e are observed at around 20 mm distance from the target. In the context of ZnO thin film formation the present investigation suggests that the films will invariably be nonstoichiometric when target is ablated in high vacuum. Ablating the target in the oxygen atmosphere and keeping the substrate beyond 10 mm from the target could improve the stoichiometry.

ACKNOWLEDGMENTS

One of the authors (K.J.S.) wishes to thank Centre of Excellence in Lasers and Optoelectronic Sciences for research fellowship and another author (N.V.J.) thanks University Grants Commission for the assistance under faculty improvement program. The authors thank the financial support from Kerala State Council for Science Technology and Environment under SARD program.

[1] T. Shiosaki, S. Ohnishi, Y. Hirokawa, and A. Kawa Bata, Appl. Phys. Lett. **33**, 406 (1978).
[2] M. Hiramatsu, K. Imaeda, N. Horio, and M. Nawata, J. Vac. Sci. Technol. A **16**, 669 (1998).
[3] H. Kim *et al.*, Appl. Phys. Lett. **76**, 259 (2000).
[4] Y. Ryu, S. Zhu, D. C. Look, J. M. Wrobel, H. M. Jeong, and H. W. White, J. Cryst. Growth **216**, 330 (2000).
[5] C. J. Lee, T. J. Lee, S. C. Lyu, Y. Zhang, H. Ruh, and H. J. Lee, Appl. Phys. Lett. **81**, 3648 (2002).
[6] R. L. Hoffman, B. J. Norris, and J. F. Wager, Appl. Phys. Lett. **82**, 733 (2003).
[7] J. Aranovich, A. Ortiz, and R. H. Bube, J. Vac. Sci. Technol. **16**, 994 (1979).
[8] B. Lin, Z. Fu, and Y. Jia, Appl. Phys. Lett. **79**, 943 (2001).
[9] F. S. Hickernell, J. Appl. Phys. **44**, 1061 (1973).
[10] G. H. Lee, Y. Yamamoto, M. Kourogi, and M. Ohtsu, Thin Solid Films **386**, 117 (2001).
[11] A. S. Riad, S. A. Mahmoud, and A. A. Ibrahim, Physica B **296**, 319 (2001).

[12]S.-H. Lim, J. Washburn, Z. Lilientalk-Weber, and D. Shindo, J. Vac. Sci. Technol. A **19**, 2601 (2001).
[13]X. W. Sun and H. S. Kwok, J. Appl. Phys. **86**, 408 (1999).
[14]H. Cao, J. Y. Wu, H. C. Ong, J. Y. Dai, and R. P. H. Chang, Appl. Phys. Lett. **73**, 572 (1998).
[15]J. Perrière, E. Millon, W. Seiler, C. Boulmer-Leborgne, V. Craciun, O. Albert, J. C. Loulergue, and J. Etchepare, J. Appl. Phys. **91**, 690 (2002).
[16]R. E. Leuchtner, Appl. Surf. Sci. **127**, 626 (1998).
[17]M. Ying, Y. Xia, Y. Sun, Q. Lu, M. Zhao, and X. Liu, Appl. Surf. Sci. **207**, 227 (2003).
[18]H. R. Griem, *Plasma Spectroscopy* (McGraw-Hill, New York, 1964).
[19]G. Bekfi, *Principles of Laser Plasmas* (Wiley, New York, 1976).
[20]J. R. Fuhr and W. L. Wiese, in *Handbook of Chemistry and Physics*, 79th Ed., edited by D. R. Lide (CRC, Boca Raton, FL, 1998), pp. 10–126 and 10–146.
[21]F. J. Gordillo-Vazquez, A. Perea, J. A. Chaos, J. Gonzalo, and C. N. Afonso, Appl. Phys. Lett. **78**, 7 (2001).
[22]A. A. Voevodin, S. J. P. Laube, S. D. Walck, J. S. Solomon, M. S. Donley, and J. S. Zabinski, J. Appl. Phys. **78**, 4123 (1995).
[23]Ya. B. Zel'dovich and Yu. P. Raizer, *Physics of Shock Waves and High-Temperature Hydrodynamic Phenomena* (Academic, New York, 1966).
[24]N. Arnold, J. Gruber, and J. Heitz, Appl. Phys. A: Mater. Sci. Process. **69**, S87 (1999).
[25]F. Claeyssens, A. Cheesman, S. J. Henley, and M. N. R. Ashfold, J. Appl. Phys. **92**, 6886 (2002).
[26]R. Manoj, A. Antony, C. Vineeth, and M. K. Jayaraj, Proceedings of DAE-BRNS National Laser Symposium (Allied Publishers, Mumbai, India, 2002), p. 423–424.
[27]P. E. Dyer, Appl. Phys. Lett. **55**, 1630 (1989).
[28]T. N. Hansen, J. Schou, and J. G. Lunney, Europhys. Lett. **40**, 441 (1997).
[29]T. N. Hansen, J. Schou, and J. G. Lunney, Appl. Phys. Lett. **72**, 1829 (1998).